A dynamic model for age-specific fertility rates in Italy

Sandra De Iaco *, Sabrina Maggio

Department of Management, Economics, Mathematics and Statistics, University of Salento, Ecotekne, Via per Monteroni, 73100 Lecce, Italy

ARTICLE INFO

Keywords:
Dynamic fertility table
Age-specific fertility rate
Spatio-temporal stochastic model
Non-separable covariance model
Jackknife prediction

ABSTRACT

Fertility evolution in Italy has shown a deep drop in 1995, and up to now the fertility rate is considered among the lowest in the world. The empirical distribution of the age-specific fertility rates is characterized by a decreasing tendency of the maximum fertility rate and a simultaneous increase of the corresponding mother's age. This tendency has been stimulating recent contributions in modelling and forecasting.

The aim of this paper is to propose a dynamic model for describing and predicting the evolution of the Italian age-specific fertility rates over time. In particular, a well-documented model, such as a Gamma function, slightly modified in order to include time-varying stochastic parameters, is used to describe the systematic and macroscopic variations of the age-specific fertility rates over time, while a nonparametric geostatistical model is applied to describe the correlated residuals at microscopic level. Finally, predictions for the variable under study are provided and main empirical evidences of the temporal evolution for different mother's ages are discussed.

Abbreviations: FR, fertility rates; GARCH, Generalized AutoRegressive Conditional Heteroskedasticity; ARCH, Autoregressive Moving Average; ARIMA, Autoregressive Integrated Moving Average; STRF, spatio-temporal random field; SE, Standard Error; ACF, autocorrelation functions; PACF, partial autocorrelation functions; nls, non-linear least squares regression; MAE, mean absolute error; RMSE, root mean square error.

* Corresponding author.
E-mail address: sandra.deiaco@unisalento.it (S. De Iaco).

http://dx.doi.org/10.1016/j.spasta.2016.05.002

1. Introduction

Several contributions on modelling and predicting fertility rates (FR) can be found in the literature. Some of them are related to the Total FR and are based on different approaches, such as GARCH (Generalized AutoRegressive Conditional Heteroskedasticity), ARCH and ARIMA (Autoregressive Integrated Moving Average) time series models (Alders and de Beer, 2004; Keilman and Pham, 2004; Lee and Tuljapurkar, 1994; Lee, 1993; Lee and Wu, 2003), Bayesian models (Raftery et al., 2014) or spatio-temporal geostatistical models (De Iaco et al., 2015). Other models provide excellent fits to the distributions of the age-specific FR referred to specific calendar years (Gayawan et al., 2010; Peristera and Kostaki, 2007) and are useful in social planning (Billari et al., 2012), for both government and private institutions (Hoem et al., 1981; Smith, 1987). Moreover, modern mixture models can capture fertility patterns which exhibit an almost bimodal shape (Chandola et al., 2002). This is common for age-specific FR distributions of developed countries, such as the United Kingdom, Ireland and USA, which are characterized by two populations with different age-specific FR (Azzalini, 1985, 2005; Mazzucco and Scarpa, 2015; Peristera and Kostaki, 2007). Unlike other developed countries, Italy has maintained a classic fertility pattern (a bell shaped distribution, roughly symmetrical though sharper in its left part of its peak) with no additional hump.

In this context, a further step in modelling is related with the possibility of considering that age-specific FR data are often given as a two-way table on a grid, equally spaced in either the vertical (calendar year) and horizontal (mother's age) directions. This type of demographic tables requires not only a temporal analytical perspective, but also a consciousness of the corresponding female age, which in this case can be interpreted as another dimension of the domain. Then, they can be suitably interpreted as data with a spatio-temporal like structure on a two-dimensional domain, i.e. the vertical (time) and horizontal (space) directions. In this case, dynamic fertility tables arise as an alternative to the standard (static) fertility table, with the aim of incorporating the evolution of fertility over time. This is consistent with recent advances in demographic research which are usually based on collection and analysis of individual- and contextual-level data across a wide range of spatial and temporal scales (Matthews and Parker, 2013; Voss, 2007; Weeks, 2004; Débon et al., 2008; Martinez-Ruiz et al., 2010). Booth (2006) offers a wide overview since 1980 about the approaches and developments in demographic forecasting. As remarked by Shang (2015), forecasting methods for age-specific FR can be organized into three classes: parametric (Thompson et al., 1989; Keilman, 2008), semi-parametric (Booth, 1984) and non-parametric models (Bozik and Bell, 1987; Lee, 1993; Hyndman and Shahid Ullah, 2007; Hyndman and Booth, 2008). Nevertheless, none of the forecasting methods in the demographic fertility literature takes into account the existing dependence structure among the data.

In this paper, a new approach in modelling and forecasting age-specific FR is proposed and applied to the Italian FR which has shown a steep decreasing tendency and is considered at the moment among the lowest in the world. The novelty of this paper is (1) to propose an appropriately modified version of an existing parametric model in order to incorporate the macroscopic variation of age-specific rates over time and (2) to treat the correlated residuals at microscopic level (which are usually ignored) by using a two-dimensional geostatistical model.

The rest of the article is organized as follows. Section 2 presents the available two-way table of the Italian age-specific FR for the period 1952–2012. In Section 3 the dynamic model with correlated residuals is introduced and the Italian trend of the age-specific FR (from 13 to 50 years old) over the temporal interval of interest, is reasonably described by a Gamma function (Hoem et al., 1981), with stochastic parameters depending on time. Thus, in Section 3.1 the time-varying stochastic parameters of the Gamma function are estimated and modelled, while in Section 3.2 the age-specific FR correlated residuals (obtained by removing the FR trend component from the observed age-specific FR) are appropriately studied through structural analysis. In Section 4 spatio-temporal kriging based on a suitable class of non-separable covariance models is applied for prediction purposes. Some empirical evidences of the FR evolution in time and for different mother's ages are discussed. Finally, a comparison between the proposed stochastic model with a correlated residual component and the traditional model, commonly used to describe only the systematic structure, is provided in Section 5.

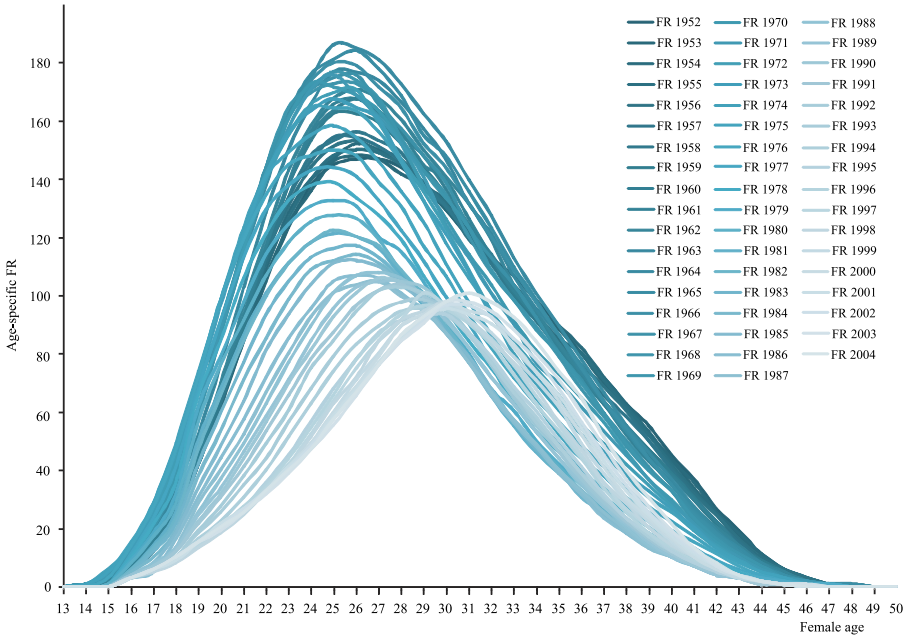

Fig. 1. Cartesian diagram of the age-specific FR from 1952 to 2004.

2. Two-way table of age-specific FR in Italy

Fertility evolution in Italy has shown a deep drop in 1995, and up to now the Italian FR is considered among the lowest in the world. This tendency has been stimulating contemporary theories of childbearing and family building and recent contributions in modelling. Italian fertility level can be partly explained by its scarce family policy that should be more incisive and capable to accommodate women entry into the labour force (Castro, 2007).

The analysed data set refers to the Italian age-specific FR corresponding to the period 1952–2012.[1] In particular, data for the last 8 years (from 2005 to 2012) have been used at first for validation purposes, then after assessing the accuracy of the model, the complete data set for the period 1952–2012 has been considered for modelling and prediction. In the following, the two-way table of the Italian age-specific FR for the period 1952–2004 has been described.

The age-specific FR, denoted with $Z(s, t)$, represents the number of births occurring during a given year t, per 1000 women, in each reproductive age s (13–50 years). This is defined as follows:

$$Z(s, t) = [B(s, t)/\bar{F}(s, t)] \cdot 1000$$

where $B(s, t)$ is the number of births to women of a specified age s during a given year t, and $\bar{F}(s, t)$ is the number of women of the same age s during the specified year t.

Fig. 1 illustrates the Cartesian diagram of the Italian age-specific FR: the distribution of the data versus the female age is characterized by positive asymmetry, which has been decreasing in the last 10 years.

It is important to highlight that the empirical distribution of the age-specific FR has changed gradually and significantly over the temporal interval 1952–2004. In particular, the decreasing tendency of the maximum FR and the simultaneous increasing tendency of the age corresponding to the maximum FR, are shown in Fig. 2.

[1] (Data sources: demo.istat.it/fecondita/index.html for the period 1952–2004 and demo.istat.it/altridati/IscrittiNascita for the period 2005–2012, published online by the Italian National Institute of Statistics.)

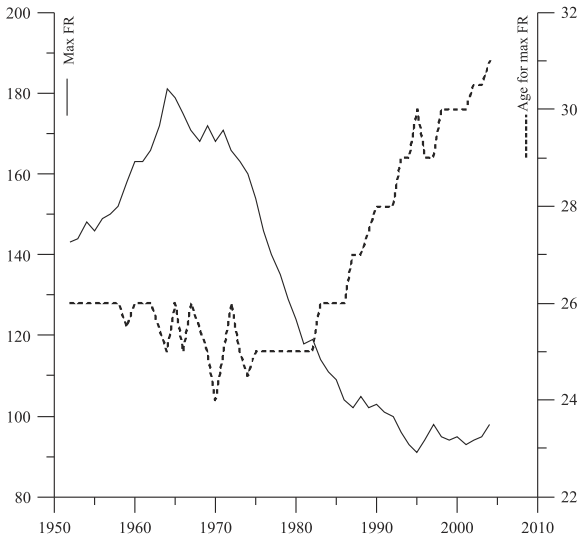

Fig. 2. Time plots of the maximum age-specific FR and the corresponding age for the period 1952–2004.

Note that peaks in the distributions occur in the age interval 25–26, for the period 1963–1971, while a rapid decrease in fertility is registered during the period 1972–1995 (especially for the age group 27–30). Finally, the fertility decline slows down in the successive period where the highest age-specific FR are recorded for women over 30. This delay in childbearing is probably associated with deferred marital status as well as higher educational levels, or with the use of contraceptive and social status of the mother, as demonstrated by various contributions (Hyndman and Shahid Ullah, 2007).

3. Dynamic model with correlated residuals

FR data, which are observed for different mother's ages and calendar years, can be naturally referred to a bidimensional domain with a spatio-temporal structure, whose horizontal direction (space) is associated with the mother's age and vertical direction (time) is associated with the calendar year.

As in many cases encountered in analysing natural processes (Monestiez et al., 2001; Myers, 2002; Skøien and Blöschl, 2006; Spadavecchia and Williams, 2009; Weissmann and Fogg, 1999), this demographic variable presents a systematic structure (trend) at macroscopic level and a residual component at microscopic level. In this case, some geostatistical tools which allow both components to be evaluated, are often convenient (Gething et al., 2006). Then, by recalling the random field theory (Yaglom, 1962), the observed values of the above mentioned FR are considered as a realization of a spatio-temporal random field (*STRF*) Z over a bidimensional domain $D \times T$, where D represents the spatial domain (mother's age) and T the temporal one (calendar year). In particular, the spatio-temporal framework is reasonable since:

- the calendar year represents naturally the time coordinate;
- the mother's age represents another dimension with respect to the calendar year and it is not directly comparable with it. It worth underlining that for a fixed mother's age, the data set of the specific FR (vertical axis) for each calendar year (horizontal axis) is a time series since data are referred to time points; on the other hand, for a fixed calendar year, the data set of the specific FR (vertical axis) for each mother's age (horizontal axis) is not a time series since data are not referred to time points;
- the mother's age has an intrinsic order, but the idea of having past, present and future is not appropriate;

- the mother's age represents a coordinate on a generic $1D$ domain. Note that a $1D$ domain is naturally isotropic, then it is essentially ordered as it is the mother's age.

The *STRF* Z is reasonably decomposed as follows:

$$Z(s,t) = M(s,t) + Y(s,t), \quad (s,t) \in D \times T, \tag{1}$$

where $M(s,t) = E[Z(s,t)]$, usually called trend or drift, describes the large-scale variations and Y describes the second order stationary residuals with zero expected value, and variogram:

$$2\gamma(h_s, h_t) = \mathrm{Var}\{Y(s,t) - Y(s+h_s, t+h_t)\}$$

where h_s and h_t are called separation lags, $(s, s+h_s) \in D^2$ and $(t, t+h_t) \in T^2$. In the literature, there are several contributions on age-specific FR models describing the systematic structure at macroscopic level (Azzalini, 1985, 2005; Billari et al., 2012; Gayawan et al., 2010; Mazzucco and Scarpa, 2015; Peristera and Kostaki, 2007). As shown in Fig. 1, the Italian fertility trend component is characterized by the following aspects: (a) the age-specific distributions exhibit a decreasing asymmetry over time, (b) decreasing FR peaks associated with simultaneous increases in the female age especially over the last forty years, (c) an overall decrease of the FR levels for all female ages. On the basis of the above mentioned empirical evidences and taking into account that, differently from other countries, Italy has maintained a classic fertility pattern (a bell shaped distribution, roughly symmetrical though sharper in its left part of its peak) with no additional hump, the following functional form for the trend has been considered:

$$M(s,t) = A_t \cdot \left\{ \frac{\upsilon^{N_t}}{\Gamma(N_t)} s^{(N_t-1)} e^{-\upsilon s} \right\}, \tag{2}$$

where A_t and N_t are stochastic positive parameters representing the proportional factor and the shape coefficient respectively, $\Gamma(\cdot)$ is a Gamma function and υ is a positive constant, called the rate parameter (the reciprocal of the scale parameter). Except for the proportional factor A_t, the trend component of the age-specific FR is described, for a fixed t, by a Gamma function with a stochastic shape parameter N_t and a rate parameter υ. This functional form, with time-varying stochastic parameters represents a revised version of the Gamma function (Hoem et al., 1981) and reproduces the main features of the Italian age-specific FR which are characterized by a bell shaped distribution, with a slightly positive asymmetry and no additional hump.

3.1. Estimation and modelling trend parameters

The trend parameters have been estimated by using the NLR algorithm in SPSS software (version 20) based on the Sequential Quadratic Programming method which is one of the most successful methods for the numerical solution of constrained nonlinear optimization problems (Nocedal and Wright, 1999, p. 527). Table 1 illustrates the parameter estimates and the corresponding standard errors (Seber and Wild, 2003, p. 21) evaluated for each year (from 1952 to 2004) through the above mentioned non-linear optimization procedure, under the bound on the constant $\upsilon = 0.63$ which guarantees the algorithm convergence. As confirmed by analysing the adjusted $\bar{R}^2$ statistic in Table 1, the age-specific FR trend, described through the function in Eq. (2), provides a good fit for each calendar year in the interval 1952–2004. At this point, the estimates, denoted with $\widehat{N}_t$ and $\widehat{A}_t$, of the stochastic parameters N_t and A_t have been analysed and modelled.

Fig. 3 shows the temporal behaviour of the estimated values for N_t and A_t. The empirical proportional factor $\widehat{A}_t$ for a fixed calendar year t ($t = 1952, \ldots, 2004$), reflects the Total FR for each year t. Indeed, the temporal behaviour of this factor shows an increasing tendency until the 70s and a well-documented decline up to the 90s. The estimates for N_t are strongly linked to the average mother's age which is characterized by a decreasing tendency until the late 70s, and a sharp increase for the subsequent years. Then, the time series of the empirical values obtained for N_t and A_t have been further studied by using the Box–Jenkins methodology (Box et al., 2013).

As illustrated in Fig. 4, the sample autocorrelation functions (ACF) for both variables tend to damp very slowly and the sample partial autocorrelation functions (PACF) decay very quickly from lag 2.

Table 1
Estimates and standard errors (SE) for the parameters N_t and A_t, obtained by fitting the model in Eq. (2), together with the adjusted $\bar{R}^2$.

t (year)	$\widehat{N}_t\,(SE)$	$\widehat{A}_t\,(SE)$	$\bar{R}^2$	t (year)	$\widehat{N}_t\,(SE)$	$\widehat{A}_t\,(SE)$	$\bar{R}^2$
1952	18.39 (0.74)	2400.17 (42.92)	0.98	1979	16.98 (1.02)	1897.32 (50.95)	0.97
1953	18.34 (0.74)	2380.01 (42.87)	0.98	1980	17.02 (1.04)	1821.03 (49.86)	0.97
1954	18.32 (0.76)	2425.88 (45.05)	0.98	1981	17.12 (1.08)	1739.54 (49.38)	0.96
1955	18.26 (0.75)	2406.39 (44.35)	0.98	1982	17.18 (1.13)	1745.62 (51.23)	0.96
1956	18.17 (0.78)	2416.59 (46.45)	0.98	1983	17.29 (1.13)	1682.11 (49.30)	0.96
1957	18.13 (0.80)	2424.61 (47.96)	0.98	1984	17.41 (1.16)	1630.70 (48.48)	0.96
1958	18.10 (0.82)	2414.83 (48.69)	0.98	1985	17.54 (1.21)	1596.39 (49.49)	0.96
1959	18.06 (0.83)	2491.46 (51.10)	0.98	1986	17.67 (1.25)	1521.17 (48.29)	0.96
1960	18.03 (0.80)	2525.13 (49.88)	0.98	1987	17.81 (1.27)	1493.04 (47.79)	0.96
1961	17.99 (0.79)	2530.09 (49.81)	0.98	1988	17.99 (1.30)	1534.27 (49.63)	0.95
1962	17.99 (0.76)	2591.28 (48.96)	0.98	1989	18.10 (1.31)	1495.98 (48.62)	0.95
1963	17.90 (0.75)	2690.74 (50.44)	0.98	1990	18.24 (1.35)	1510.35 (49.97)	0.95
1964	17.83 (0.71)	2835.07 (50.26)	0.98	1991	18.33 (1.35)	1477.75 (48.53)	0.95
1965	17.73 (0.73)	2791.22 (51.52)	0.98	1992	18.48 (1.42)	1466.49 (50.54)	0.95
1966	17.71 (0.77)	2744.78 (53.55)	0.98	1993	18.60 (1.44)	1407.60 (48.76)	0.95
1967	17.61 (0.82)	2658.56 (55.45)	0.98	1994	18.74 (1.51)	1361.63 (49.11)	0.94
1968	17.54 (0.86)	2612.60 (57.18)	0.98	1995	18.94 (1.63)	1332.14 (51.15)	0.94
1969	17.56 (0.89)	2630.73 (59.42)	0.97	1996	19.05 (1.67)	1363.35 (53.40)	0.93
1970	17.44 (0.88)	2544.66 (57.77)	0.97	1997	19.17 (1.72)	1372.93 (54.87)	0.93
1971	17.39 (0.86)	2530.95 (56.38)	0.98	1998	19.25 (1.73)	1362.88 (54.67)	0.93
1972	17.27 (0.82)	2478.02 (53.00)	0.98	1999	19.34 (1.71)	1373.02 (53.98)	0.93
1973	17.19 (0.80)	2458.19 (51.17)	0.98	2000	19.42 (1.72)	1396.67 (55.23)	0.93
1974	17.11 (0.76)	2444.29 (48.82)	0.98	2001	19.49 (1.65)	1388.08 (52.49)	0.94
1975	17.00 (0.79)	2318.22 (48.41)	0.98	2002	19.58 (1.70)	1406.29 (54.29)	0.93
1976	16.95 (0.81)	2220.52 (47.83)	0.98	2003	19.69 (1.74)	1424.47 (56.12)	0.93
1977	16.94 (0.92)	2100.11 (51.23)	0.97	2004	19.76 (1.74)	1471.17 (57.66)	0.93
1978	16.96 (0.96)	2001.90 (50.80)	0.97				

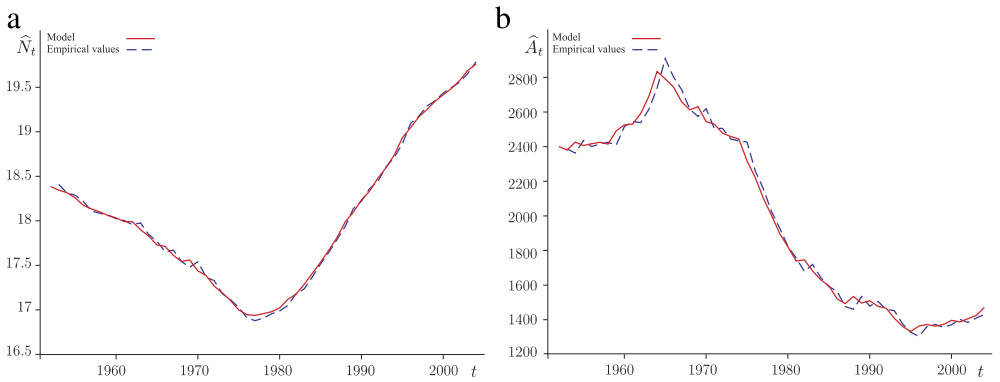

Fig. 3. Time plots for the estimates (dashed line) of (a) N_t and (b) A_t and the corresponding theoretical values (solid line) obtained through the fitted ARIMA models.

This behaviour confirms that the two time series are finite realizations of non-stationary stochastic processes. First order differences have been computed and the cointegration test of Engle and Granger (1987) has been applied. Although the unit-root hypothesis is not rejected for the individual variables, there is no evidence for cointegrated relationship since the unit-root hypothesis is not rejected for the residuals from the cointegrating regression. Taking into account the ACF and PACF behaviour, both time series have been modelled through an ARIMA model, where the order of integration is equal to 1, the order of the autoregressive component is equal to 1 and the order of the moving average component is set equal to 1, i.e.:

$$\Phi(B)(1-B)\,N_t = \Theta(B)\,U_t \qquad \Phi'(B)(1-B)\,A_t = \Theta'(B)\,U'_t$$

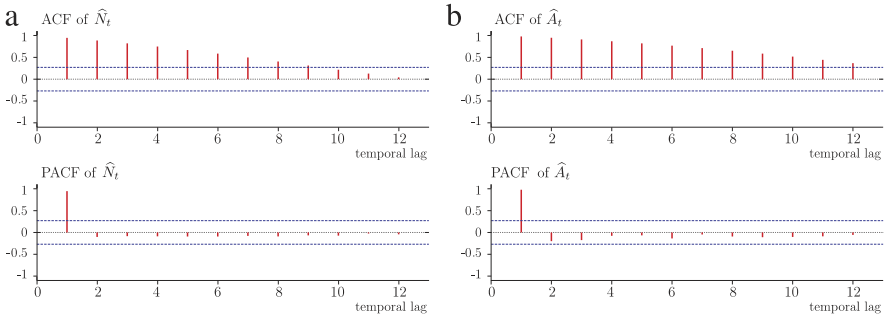

Fig. 4. Sample ACF and PACF with 95% confidence intervals (dotted line) for the estimates of (a) N_t and (b) A_t.

Table 2
ARIMA model results for N_t and A_t, for the period 1952–2004.

Variable	Parameter	Estimate	Std. Error	p-value
N_t	ϕ	0.964	0.031	<0.0001
	θ	−0.442	0.102	<0.0001
A_t	ϕ'	0.849	0.112	<0.0001
	θ'	−0.458	0.20	0.0241

where $\Phi(B)$ and $\Theta(B)$ with parameter ϕ and θ, respectively, are polynomials of the first order in the lag operator B, similarly for $\Phi'(B)$ and $\Theta'(B)$ with parameter ϕ' and θ', respectively, while U and U' are white noise random processes with variances σ_U^2 and $\sigma_{U'}^2$ respectively.

Table 2 reports the parameter estimates of (ϕ, θ) for the model of N_t and (ϕ', θ') for the model of A_t and the standard errors. Moreover, the associated p-values support the assumption that the parameters are statistically significant.

Fig. 3 illustrates the time plots of the empirical values for N_t and A_t, together with the corresponding theoretical values obtained through the ARIMA models. Apart from the visual detection of the good fitting, the selected ARIMA models have passed the residual diagnostics: the zero mean hypotheses for both the residuals are not rejected and the correlograms and the Ljung–Box statistics indicate that the residuals behave as white noise processes. Thus, the reliability of ARIMA models for N_t and A_t supports their application for prediction purposes. In other terms, the fitted models can be used to estimate the values for the parameters N_t and A_t for time points in the future, and then to evaluate the fertility trend, as in Eq. (2), for different mother's ages and future calendar years.

In conclusions, it is worth highlighting that differently from other age-specific FR models proposed in the literature, the trend model in Eq. (2) is based on a Gamma function where N_t and A_t are stochastic coefficients and its dependence from both the mother's age and the calendar year is explicitly expressed.

3.2. Structural analysis and modelling for FR residuals

Given the Italian age-specific FR over time, which represents a finite realization of the *STRF Z* in Eq. (1), the correlated residuals Y are obtained by removing the trend component, as in Eq. (2), from the observed age-specific FR. Fig. 5 illustrates the 2*D* view of the above mentioned age-specific FR residuals. As clarified, this *STRF Y* is able to capture the small-scale variations, which sometimes are erroneously treated as uncorrelated residuals.

In this context structural analysis is developed for the 2*D* FR residuals available from 1952 to 2004 (called temporal dimension) and for different mother's age (called spatial dimension), and a suitable variogram model of the residuals is identified and used for prediction purposes by applying kriging (Journel and Huijbregts, 1981). Regarding the computational aspects, predictions have been obtained by using the program *K2ST*, which is a modified GSLib routine (De Iaco and Posa, 2012).

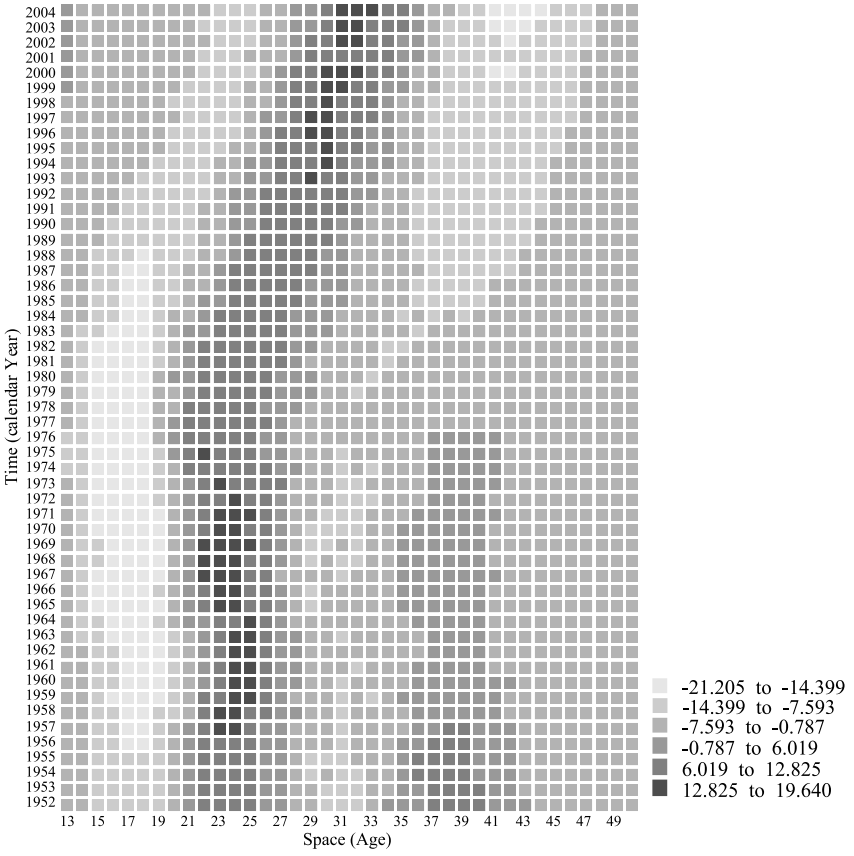

Fig. 5. 2*D* perspective of the table of age-specific FR residuals in Italy from 1952 to 2004.

Note that, after producing the predictions for the residuals through ordinary kriging, the trend component has to be added to the residuals in order to obtain the predicted age-specific FR.

3.2.1. Structural analysis

Structural analysis begins with the estimation of the variogram of the *STRF* Y in Eq. (1), over the set of data locations $A = \{(s, t)_i,\ i = 1, 2, \ldots, n\}$, where the coordinate s is associated with the mother's age and t is associated with the calendar year. Then, the sample variogram $\widehat{\gamma}$ is evaluated as follows:

$$\widehat{\gamma}(h_s, h_t) = \frac{1}{2|L(h_s, h_t)|} \sum_{L(h_s,h_t)} \{Y(s + h_s, t + h_t) - Y(s, t)\}^2, \tag{3}$$

where $|L(h_s, h_t)|$ is the cardinality of $L(h_s, h_t) = \{(s + h_s, t + h_t) \in A, (s, t) \in A\}$.

It is important to highlight that no metric is defined in the 2*D* domain. Indeed, the pairs of points separated by (h_s, h_t) are detected by computing, separately, the distances (in terms of age and year); thus, the pairs of realizations, $y(s, t)$ and $y(s+h_s, t+h_t)$, correspond to points that are simultaneously separated by h_s in the spatial domain or horizontal direction (mother's age), and h_t in the temporal domain or vertical direction (calendar year). On the basis of the above-mentioned interpretation, we will use the expression "space–time variogram". The sample space–time variogram for the age-specific FR residuals has been determined and shown in Fig. 6(a).

The variogram surface reflects a well-structured correlation, which is high for small lags (h_s, h_t) and it is lower and lower for greater lags.

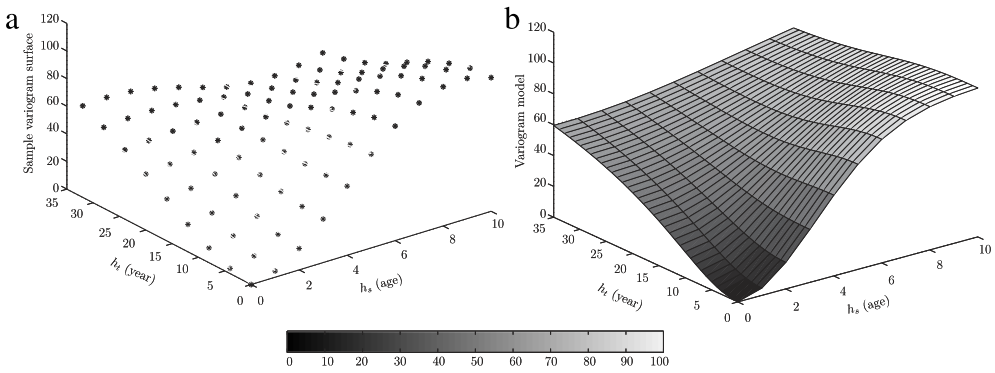

Fig. 6. (a) Sample variogram surface, (b) variogram model of the age-specific FR residuals.

The second step of structural analysis consists in choosing a theoretical admissible model (Christakos, 1984) and fitting it to the sample space–time variogram. In literature, various admissible variogram models are available; one can choose between separable or non-separable variogram models, where the former models are based on the assumption that the two dimensions of the domain are independent and the latter models are based on the assumption that there exists an interaction factor. Recently, different forms of non-separability have also been defined and wide classes of non-separable variogram models have been classified according to these characteristics (De Iaco and Posa, 2013). Indeed, the selection of the appropriate class of models for the age-specific FR residuals has been based on the geometric features of the empirical variogram surface and some properties, such as the type of non-separability (De Iaco et al., 2013). Thus, the following spatio-temporal variogram model, belonging to the Gneiting class (Gneiting et al., 2002), has been chosen:

$$\gamma\left(h_s, h_t; \boldsymbol{\Theta}\right) = \begin{cases} 0 & (h_s, h_t) = 0 \\ N + C\left[1 - \left\{\dfrac{1}{\left(a \cdot h_t^{2\alpha} + 1\right)^{\tau}}\right\} \cdot \exp\left\{-\dfrac{c \cdot h_s^{2\gamma}}{\left(a \cdot h_t^{2\alpha} + 1\right)^{\beta\gamma}}\right\}\right] & \text{otherwise} \end{cases} \tag{4}$$

where $\boldsymbol{\Theta} = (N, C, a, c, \alpha, \tau, \gamma, \beta)$ with $N, C, a \geq 0, c \in \mathbb{R}, \tau \geq 0.5$ (for $1D$ spatial dimension), $\alpha, \gamma \in (0, 1], \beta \in [0, 1]$; this non-separable model allows the interaction between FR specified by age and their temporal evolution to be considered. The above Gneiting model has been fitted through non-linear least squares estimation (Cressie, 1985), based on the following function:

$$W\left(\boldsymbol{\Theta}\right) = \sum_{L(h_s, h_t)} L\left(h_s, h_t\right) \cdot \left\{\frac{\widehat{\gamma}\left(h_s, h_t\right)}{\gamma\left(h_s, h_t; \boldsymbol{\Theta}\right)} - 1\right\}^2. \tag{5}$$

In particular, the parameters a, c, N, C and β of the above model have been estimated through the S-Plus function *nls* (non-linear least squares regression). The remaining parameters have been easily fixed through the visual inspection of the sample variogram surface. The smoothness parameters α and γ, as well as the parameter τ, have been set equal to 1, on the basis of the parabolic behaviour of the sample variogram near the origin along the spatial and temporal profile. Fig. 6(b) illustrates the fitted Gneiting model in Eq. (4), with $\boldsymbol{\Theta} = [0.21232, 97.168, 0.0045606, 0.048146, 1, 1, 1, 0.9438]$. Note that the relative mean square error (corresponding to the minimum value of $W\left(\boldsymbol{\Theta}\right)$ divided by the total number of pairs in the set $L\left(h_s, h_t\right)$, for all h_s and h_t), is equal to 0.019, while the square root of the relative mean square error is equal to 0.136. These values provide a measure of the goodness of fit and support the choice of the non-separable model given in Eq. (4).

In the following section, a further validation of the space–time variogram model has been proposed; then, the validated model has been used for yearly predictions.

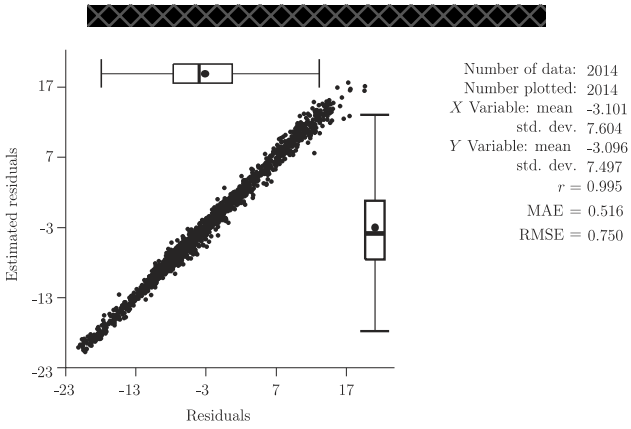

Fig. 7. Scatter plot of the residuals of observed age-specific FR versus the residuals of estimated FR from 1952 to 2004, obtained through cross-validation.

Table 3
Predicted values of N_t and A_t obtained through the fitted ARIMA models for (a) the period 2005–2012, (b) the period 2013–2025.

(a)			(b)					
t (year)	$\widehat{N}_t$	$\widehat{A}_t$	t (year)	$\widehat{N}_t$	$\widehat{A}_t$	t (year)	$\widehat{N}_t$	$\widehat{A}_t$
2005	19.841	1489.201	2013	20.099	1544.940	2021	20.233	1498.244
2006	19.919	1501.257	2014	20.116	1543.853	2022	20.249	1488.595
2007	19.994	1508.457	2015	20.134	1540.893	2023	20.264	1478.521
2008	20.068	1511.715	2016	20.151	1536.376	2024	20.280	1468.093
2009	20.140	1511.773	2017	20.168	1530.565	2025	20.295	1457.371
2010	20.210	1509.233	2018	20.184	1523.680			
2011	20.278	1504.583	2019	20.201	1515.902			
2012	20.344	1498.220	2020	20.217	1507.381			

3.2.2. Model validation

In the previous section, a suitable space–time variogram model has been fitted to the empirical variogram surface of the age-specific FR residuals; as a subsequent step the reliability of the fitted model in Eq. (4) has been evaluated through the application of cross-validation and jackknife techniques. Some statistical tools based on the comparison between estimates and sample data, have been used to evaluate the goodness of the fitted model. Among these, the mean absolute error (MAE) and the root mean square error (RMSE) between the true values and the estimated ones have been computed and the test of the null hypothesis that the difference between the true mean value and the estimated one is equal to zero has also been conducted. Afterwards, the space–time kriging based on the same model in Eq. (4) has been used to predict the age-specific FR for future time points.

Cross-validation results have been represented through the scatter plot between observed values and estimates, and appropriately summarized (Fig. 7). The comparison between the descriptive statistics computed for the residuals of observed age-specific FR and the estimated rates, together with the correlation coefficient (equal to 0.995) encourage the use of model in Eq. (4) for prediction purposes. Moreover, this is also confirmed by analysing the box plots of the observed and estimated FR residuals (Fig. 7).

In addition, the jackknife kriging predictions for the age-specific FR from 2005 to 2012 have been also computed by using the above fitted model and by considering the residuals up to 2004. In this way, after predicting the residuals for the period 2005–2012, the trend values of the same period have been added to the jackknife predicted residuals in order to obtain the age-specific FR predictions. Note that, for this aim, the stochastic parameters of the trend model in Eq. (2) have also been predicted for the period 2005–2012 through the corresponding ARIMA models discussed in Section 3. Table 3(a) reports the predicted values for these parameters.

Then the observed age-specific FR from 2005 to 2012 (which were available but not used in the previous structural analysis) have been compared with the predicted ones. Figs. 8–9 illustrate the main

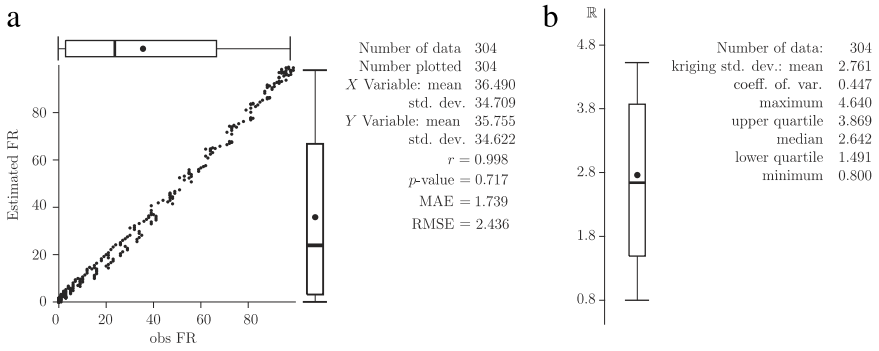

Fig. 8. (a) Scatter plot of the observed age-specific FR versus the estimated FR for the period 2005–2012, (b) box plot of the square root of the error variance estimations.

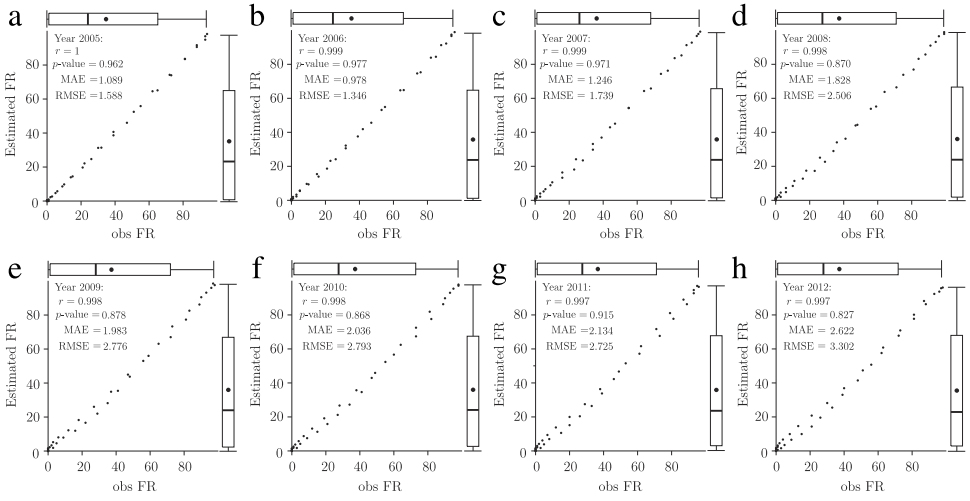

Fig. 9. Scatter plots of the observed age-specific FR versus the estimated FR from 2005 to 2012 (a–h).

results obtained from jackknife technique. It is worth noting that the predicted FR values reproduce very well the observed FR data, as shown in Fig. 8(a). Moreover, the correlation coefficient computed between the observed FR and the predicted ones is close to 1 (0.998) and the *p*-values related to the test of the null hypothesis that the difference between true mean value and estimated mean value is equal to zero, leads to the acceptance of the test.

Fig. 8(b) illustrates the box plot of the kriging standard deviation (i.e. square root of error variance estimation). It is evident that the corresponding frequency distribution is approximately symmetric and is characterized by low variability. Note that the scatter plots of the observed age-specific FR versus the estimated FR, evaluated for each year from 2005 to 2012 (Fig. 9), confirm the results obtained from the analysis performed on the eight-year period (Fig. 8). These results and other statistics such as the MAE and the RMSE (5%–7% of the FR mean), as well as the *p*-values for the tests on the estimations errors, also reflect the reliability of the kriging estimates.

4. Predictions of the Italian age-specific FR

Given the variogram model in Eq. (4), spatio-temporal kriging has been properly applied in order to obtain predictions of the specific FR residuals for each mother's age, from 13 to 50 years old, over the period 2013–2025. Then, the age-specific FR predicted values for the period 2013–2025 have been

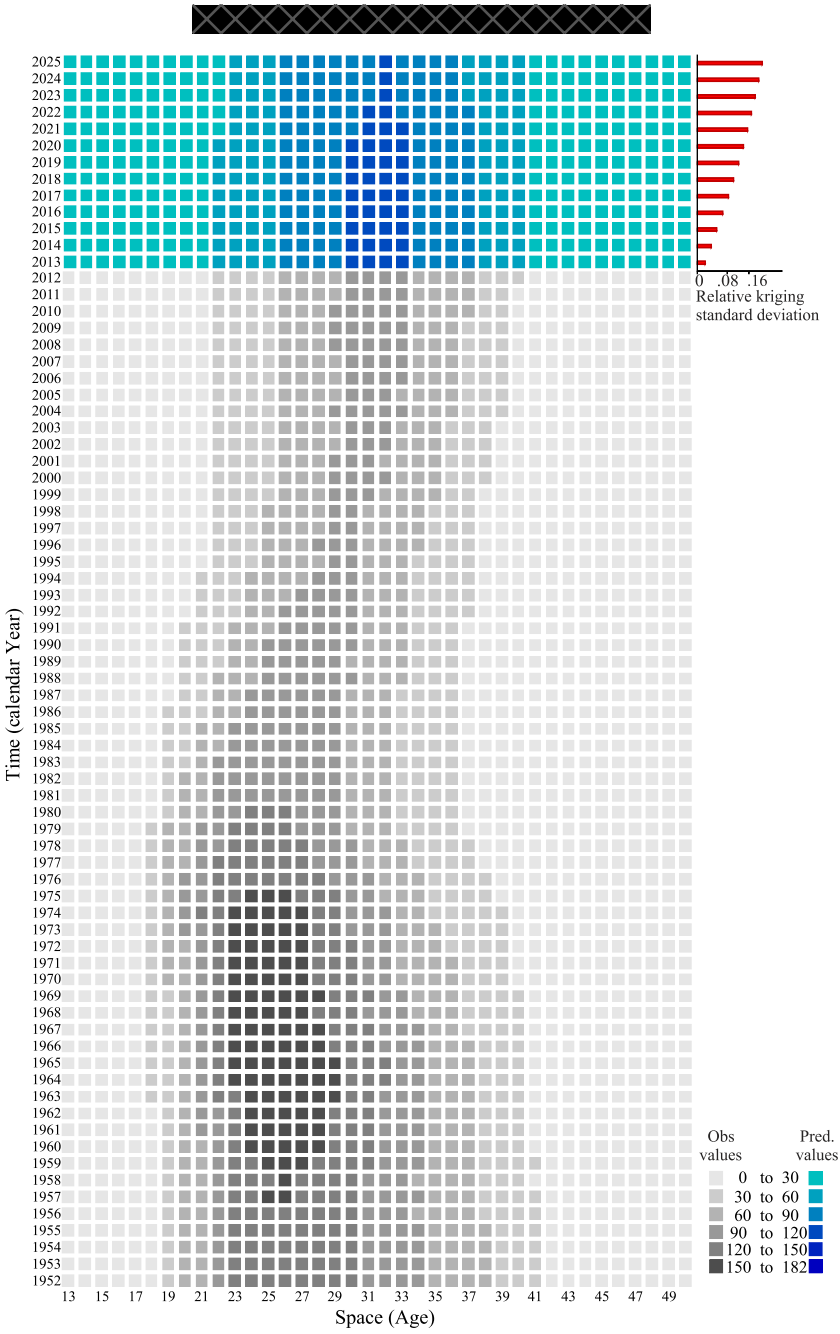

Fig. 10. Space–time perspective of the table of fertility in Italy from 1952 to 2012, together with the predicted values and their relative kriging standard deviations from 2013 to 2025.

obtained by adding the predicted residuals to the trend components based on the model in Eq. (2) and on the parameter estimates in Table 3(b).

The 2*D* perspective of the observed age-specific FR from 1952 to 2012 together with the predicted age-specific FR from 2013 to 2025 and their relative kriging standard deviations (i.e. square root of the kriging error variance per FR unit) is shown in Fig. 10. It is evident that the age-specific FR tends to

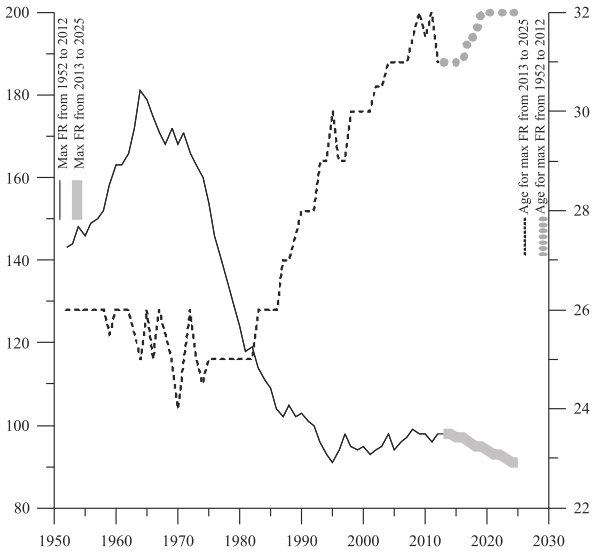

Fig. 11. Time plots of the maximum FR and the corresponding age for the period 1952–2004, together with the predicted maximum FR for the women (continuous thick line) and mother's age corresponding to the maximum FR (dashed thick line) from 2013 to 2025.

be, on average, lower with respect to the previous period, the asymmetry decreases over time and the maximum values tend to be more concentrated around the age interval of 31–33 years old up to 2022 and at the age of 32 years old for the following three years. The relative kriging standard deviations, averaged over the mother's age, for the period 2013–2025 show an increasing tendency over time, although it is very slow (0.009 per year). This suggests that predictions can be considered reliable up to the end of the estimation period.

The time plots of the maximum FR and the corresponding mother's age for the period 1952–2025 are shown in Fig. 11. Note that the maximum FR for the women will continue decreasing slowly from 2013 to 2025 (continuous thick line), while the mother's age corresponding to the maximum FR (dashed thick line) is going to stabilize around 32 years old. This trend is much more evident by considering the predicted values from 2013 to 2025 shown in Table 4.

This perspective should stimulate more incisive family policies which should support childbearing as well as financial assistance and tax reliefs.

5. A comparative analysis

The use of the proposed dynamic model can be justified and supported on the basis of a comparative analysis. The comparison has been conducted with respect to the traditional Gamma model (Hoem et al., 1981), which is widely used to describe the systematic structure of the age-specific FR. In the following, some inferential tests have been proposed and discussed. First of all, it has been worth testing if predictions can be significantly improved when the new dynamic model with correlated residuals is used instead of the traditional model, which enables for describing only the macroscopic variations of the variable under study. Thus, given the null hypothesis that the difference between the absolute estimation errors, obtained through the traditional model, and the absolute errors, obtained through the new model, is on average less than zero, a one-tailed test on the right has been performed. Note that this test has been conducted for the period 2005–2012, for which true values are available and the estimated errors can be computed.

The importance of using the proposed stochastic model with correlated residuals is proved by the rejection of the null hypothesis at a 5% significance level: indeed, the p-value corresponds to 1.33E−39 (<0.05).

Table 4
Predictions for the age-specific FR in Italy from 2013 to 2025.

Age	Calendar year												
	2013	2014	2015	2016	2017	2018	2019	2020	2021	2022	2023	2024	2025
13	0	0	0	0	0	0	0	0	0	0	0	0	0
14	0	0	0	0	0	0	0	0	0	0	0	0	0
15	1	1	1	1	1	1	1	1	1	1	1	1	1
16	2	2	2	2	2	2	2	2	2	2	2	2	2
17	5	5	5	5	5	5	5	4	4	4	4	4	4
18	9	9	9	9	8	8	8	8	8	8	8	8	8
19	14	14	14	14	13	13	13	12	12	12	11	11	11
20	20	20	20	19	19	19	18	18	17	17	16	16	15
21	26	26	26	25	25	24	24	23	23	22	22	21	21
22	32	32	32	32	31	31	31	30	30	30	29	29	28
23	39	39	39	39	38	38	38	37	37	37	36	36	36
24	48	47	47	46	46	46	45	45	45	44	44	44	43
25	56	55	55	55	54	54	54	53	53	53	52	52	51
26	64	64	63	63	63	63	63	62	62	62	61	61	61
27	73	72	72	72	72	71	71	71	70	70	69	69	68
28	81	81	80	80	80	80	79	79	79	78	78	77	77
29	88	88	88	88	87	87	87	86	86	85	84	84	83
30	95	95	94	94	93	92	92	91	90	89	88	87	87
31	98	98	97	97	96	95	94	93	92	91	90	89	88
32	97	97	96	96	96	95	95	94	93	93	92	91	91
33	93	93	93	93	92	92	92	91	90	90	89	88	88
34	88	88	88	88	87	87	86	86	85	85	84	83	83
35	80	81	81	81	80	80	79	79	78	78	77	76	76
36	71	72	72	72	72	71	71	71	70	70	69	69	68
37	62	62	62	62	62	61	61	61	60	60	60	59	59
38	51	51	51	51	51	51	51	51	51	50	50	50	50
39	41	40	41	41	41	41	41	41	41	41	40	40	40
40	31	30	31	31	31	31	31	31	31	31	31	31	31
41	21	21	21	22	22	22	22	22	23	23	23	23	23
42	13	13	14	14	14	15	15	15	16	16	16	17	17
43	8	8	8	9	9	9	10	10	10	10	11	11	11
44	5	5	5	5	5	5	6	6	6	6	6	6	6
45	3	3	3	3	3	3	3	3	3	4	4	4	4
46	1	2	2	2	2	2	2	2	2	2	2	2	2
47	1	1	1	1	1	1	1	1	1	1	1	1	1
48	0	1	1	1	1	1	1	1	1	1	1	1	0
49	0	1	1	1	0	0	0	0	0	0	0	0	0
50	0	1	1	1	0	0	0	0	0	0	0	0	0

After this step, the predictions based on the traditional Gamma model (2) and the new dynamic model have been compared for the period 2013–2025. In Fig. 12, the histogram of the differences between the predictions obtained through the use of the traditional model and the new proposed model, is illustrated. A two-tail test has also been performed on the null hypothesis that this difference is on average equal to zero; this hypothesis corresponds to the assumption that the two models lead to the same results, in terms of predictions. The null hypothesis has been rejected, as confirmed by the low p-value 2.23E−19 (<0.05) shown in Fig. 12.

6. Conclusions

In this paper, a stochastic model for the age-specific FR in Italy was proposed and the application of such a model for forecasting purposes was presented and compared with respect to the use of the traditional Gamma model. The advantage of this model is that it does not take apart the effects of both calendar year and mother age. In particular, macro-scale variations related to the presence of a FR trend over the domain and micro-scale variations of the residuals which are characterized by a strong correlation were both analysed. It is important to highlight that although the Gamma function reflects the main characteristics of the variable under study and the validation results support this

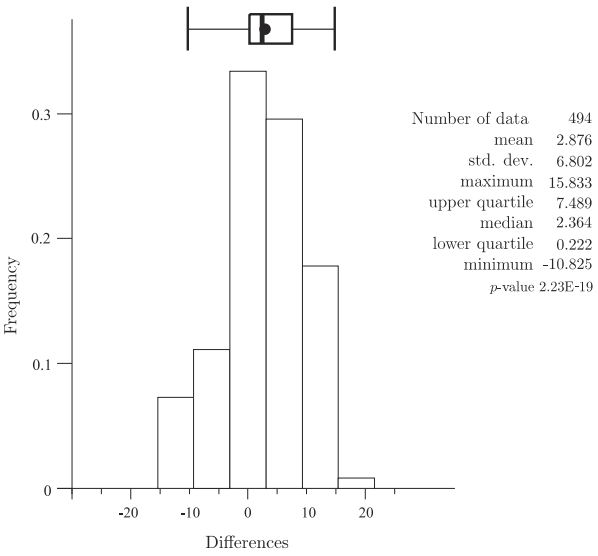

Fig. 12. Histogram of the differences between the age-specific FR predictions based on the traditional model and the predictions based on the dynamic model with correlated residuals, for the period 2013–2025.

choice, further developments might consider the use of other functional forms for the trend, such as the one proposed by Mazzucco and Scarpa (2015).

After removing the large-scale trend from the observed age-specific FR, structural analysis was developed for the correlated residuals in order to identify a suitable variogram model to be used for prediction purposes. In particular, a non-separable variogram model (such as the Gneiting class of models) which allows the users to take into account the interaction between mother's age (spatial coordinate) and calendar year (temporal coordinate), was fitted and applied in the prediction process.

On the basis of prediction results, the maximum FR will continue decreasing from 2013 to 2025, while the mother's age corresponding to the maximum FR is going to stabilize around 32 years old. This evidence should encourage the adoption of special measures to support family building and childbearing.

At last, it is worth underlining that this kind of approach lets foresee new fields of application for spatial and spatio-temporal statistics, which can be extended to a more general frame, where observations are referred to a coordinate system, which is not strictly related to a geographic system.

References

Alders, M., de Beer, J., 2004. Assumptions on fertility in stochastic population forecasts. Internat. Statist. Rev. 72, 65–79.
Azzalini, A., 1985. A class of distributions which includes the normal ones. Scand. J. Stat. 12, 171–178.
Azzalini, A., 2005. The skew-normal distribution and related multivariate families. Scand. J. Stat. 32, 159–200.
Billari, F.C., Graziani, R., Melilli, E., 2012. Stochastic population forecasts based on conditional expert opinions. J. R. Stat. Soc. Ser. A Stat. Soc. 175, 491–511.
Booth, H., 1984. Transforming Gompertz's function for fertility analysis: the development of a standard for the relational Gompertz function. Popul. Stud. 38 (3), 495–506.
Booth, H., 2006. Demographic forecasting: 1980–2005 in review. Int. J. Forecast. 22 (3), 547–581.
Box, G.E.P., Jenkins, G.M., Reinsel, G.C., 2013. Time Series Analysis: Forecasting and Control. John Wiley & Sons Inc.

Bozik, J.E., Bell, W.R., 1987. Forecasting age specific fertility using principal components. In: Proceedings of the American Statistical Association. Social Statistics Section, San Francisco, CA. pp. 396–401.
Castro, M., 2007. Spatial demography: An opportunity to improve policy making at diverse decision levels. Popul. Res. Policy Rev. 26, 477–509.
Chandola, T., Coleman, D.A., Hiorns, R.W., 2002. Distinctive features of age-specific fertility profiles in the English-speaking world: common patterns in Australia, Canada, New Zealand and the United States, 1970–98. Popul. Stud.(Camb) 56, 181–200.
Christakos, G., 1984. On the problem of permissible covariance and variogram models. Water Resour. Res. 20, 251–265.
Cressie, N.A.C., 1985. Fitting variogram models by weighted least squares. Math. Geol. 17, 563–570.
Débon, A., Montes, F., Mateu, J., Porcu, E., Bevilacqua, M., 2008. Modelling residuals dependence in dynamic life tables: A geostatistical approach. Comput. Statist. Data Anal. 52 (6), 3128–3147.
De Iaco, S., Palma, M., Posa, D., 2015. Spatio-temporal geostatistical modeling for French fertility predictions. Spat. Stat. 14 (part C), 546–562.
De Iaco, S., Posa, D., 2012. Predicting spatio-temporal random fields: some computational aspects. Comput. Geosci. 41, 12–24.
De Iaco, S., Posa, D., 2013. Positive and negative non-separability for space–time covariance models. J. Statist. Plann. Inference 143, 378–391.
De Iaco, S., Posa, D., Myers, D.E., 2013. Characteristics of some classes of space–time covariance functions. J. Statist. Plann. Inference 143, 2002–2015.
Engle, R.F., Granger, C.W.J., 1987. Co-integration and error correction: Representation, estimation, and testing. Econometrica 55, 251–276.
Gayawan, E., Adebayo, S.B., Ipinyomi, R.A., Oyejola, B.A., 2010. Modeling fertility curves in Africa. Demogr. Res. 22, 211–236.
Gething, P.W., Noor, A.M., Gikandi, P.W., Ogara, E.A.A., Hay, S.I., Nixon, M.S., 2006. Improving imperfect data from health management information systems in Africa using space–time geostatistics. PLoS Med. 3, 825–831.
Gneiting, T., 2002. Nonseparable, stationary covariance functions for space–time data. J. Amer. Statist. Assoc. 97, 590–600.
Hoem, J.M., Madsen, D., Nielsen, J.L., Ohlsen, E., Hansen, H.O., Rennermalm, B., 1981. Experiments in modelling recent Danish fertility curves. Demography 18, 231–244.
Hyndman, R.J., Booth, H., 2008. Stochastic population forecasts using functional data models for mortality, fertility and migration. Int. J. Forecast. 24 (3), 323–342.
Hyndman, R.J., Shahid Ullah, Md., 2007. Robust forecasting of mortality and fertility rates: A functional data approach. Comput. Statist. Data Anal. 51, 4942–4956.
Keilman, N., 2008. European demographic forecasts have not become more accurate over the past 25 years. Popul. Dev. Rev. 34 (1), 137–153.
Keilman, N., Pham, D.Q., 2004. Time series based errors and empirical errors in fertility forecasts in the nordic countries. Internat. Statist. Rev. 72, 5–18.
Journel, A.G., Huijbregts, Ch.J., 1981. Mining Geostatistics. Academic Press, London.
Lee, R.D., 1993. Modeling and forecasting the time series of US fertility: Age, distribution, range, and ultimate level. Int. J. Forecast. 9 (2), 187–202.
Lee, R.D., Tuljapurkar, S., 1994. Stochastic population forecasts for the United States: Beyond high, medium, and low. J. Amer. Statist. Assoc. 89, 1175–1189.
Lee, R.D., Wu, Z., 2003. Forecasting Cohort incomplete fertility: A method and an application. Popul. Stud. 57 (3), 303–320.
Martinez-Ruiz, F., Mateu, J., Montes, F., Porcu, E., 2010. Mortality risk assessment through stationary space–time covariance functions. Stoch. Environ. Res. Risk Assess. 24, 519–526.
Matthews, S.A., Parker, D.M., 2013. Progress in spatial demography. Demogr. Res. 28, 271–312.
Mazzucco, S., Scarpa, B., 2015. Fitting age-specific fertility rates by a flexible generalized skew normal probability density function. J. R. Stat. Soc. Ser. A Stat. Soc. 178 (1), 187–203.
Monestiez, P., Courault, D., Allard, D., Ruget, F., 2001. Spatial interpolation of air temperature using environmental context: Application to a crop model. Environ. Ecol. Stat. 8, 297–309.
Myers, D.E., 2002. Space–time correlation models and contaminant plumes. Environmetrics 13, 535–553.
Nocedal, J., Wright, S.J., 1999. Numerical Optimization. Springer-Verlag New York, Inc., New York.
Peristera, P., Kostaki, A., 2007. Modeling fertility in modern populations. Demogr. Res. 16, 141–194.
Raftery, A.E., Alkema, L., Gerland, P., 2014. Bayesian population projections for the United Nations. Statist. Sci. 29, 58–68.
Seber, G.A.F., Wild, C.J., 2003. Nonlinear Regression. John Wiley & Sons, Inc., Hoboken, New Jersey.
Shang, H.L., 2015. Selection of the optimal Box–Cox transformation parameter for modelling and forecasting age-specific fertility. J. Popul. Res. 32 (1), 69–79.
Skøien, J.O., Blöschl, G., 2006. Catchments as space–time filters—a joint spatio-temporal geostatistical analysis of runoff and precipitation. Hydrol. Earth Syst. Sci. 10, 645–662.
Smith, S.K., 1987. Tests of forecast accuracy and bias for county population projections. J. Amer. Statist. Assoc. 82, 991–1003.
Spadavecchia, L., Williams, M., 2009. Can spatio-temporal geostatistical methods improve high resolution regionalisation of meteorological variables? Agric. For. Meteorol. 149, 1105–1117.
Thompson, P.A., Bell, W.R., Long, J.F., Miller, R.B., 1989. Multivariate time series projections of parameterized age-specific fertility rates. J. Amer. Statist. Assoc. 84 (407), 689–699.
Voss, P.R., 2007. Demography as a spatial social science. Popul. Res. Policy Rev. 26, 457–476.
Weeks, J.R., 2004. The role of spatial analysis in demographic research. In: Goodchild, M.F., Janelle, D.G. (Eds.), Spatially Integrated Social Science, 19. Oxford University Press, New York, pp. 381–399.
Weissmann, G.S., Fogg, G.E., 1999. Multi-scale alluvial fan heterogeneity modeled with transition probability geostatistics in a sequence stratigraphic framework. J. Hydrol. 226, 48–65.
Yaglom, A.M., 1962. An Introduction to the Theory of Stationary Random Functions. Prentice Hall Inc.